

Direct Determination of the Membrane Affinities of Individual Amino Acids<sup>†</sup>Thorgeir E. Thorgeirsson,<sup>‡</sup> Charles J. Russell,<sup>‡</sup> David S. King,<sup>§</sup> and Yeon-Kyun Shin<sup>\*‡</sup>*Department of Chemistry, University of California, Berkeley, California 94720, and Howard Hughes Medical Institute and Department of Molecular and Cell Biology, University of California, Berkeley, California 94720**Received September 26, 1995; Revised Manuscript Received November 30, 1995<sup>®</sup>*

**ABSTRACT:** Amino acids have distinct lipid bilayer affinities which influence the insertion and topology of membrane-bound polypeptides and proteins. To measure membrane affinities, 14 uncharged amino acids were introduced individually at a guest site in a 25-residue peptide derived from the membrane-binding presequence of yeast cytochrome *c* oxidase, and the peptides were labeled with a nitroxide spin-label. The free energies of transfer from phospholipid bilayers to water ( $\Delta\Delta G_{\text{bilayer}}$ ) were determined directly by examination of partitioning into phospholipid bilayers using electron paramagnetic resonance. The  $\Delta\Delta G_{\text{bilayer}}$  values are in agreement with hydrophobicities assessed from 1-octanol–water partitioning of *N*-acetyl amino acid amides [Fauchere, J.-L., & Pliska, V. (1983) *Eur. J. Med. Chem.* 18, 369–375; Eisenberg, D., & McLachlan, A. (1986) *Nature* 319, 199–203] and quantitatively demonstrate the role of the hydrophobic effect in membrane–protein interactions.

While the aversion of nonpolar amino acids for water leads to the formation of the hydrophobic core of water-soluble proteins (Kauzmann, 1959), the more favorable interactions between nonpolar amino acids and the surrounding lipid bilayer are responsible for the “inside-out” organization of membrane proteins (Engelman & Zacchai, 1980; Diesenhofer *et al.*, 1985; Rees *et al.*, 1989). To understand the forces governing the folding of membrane proteins, it is necessary to know the affinities of individual amino acids for the lipid bilayer as well as their affinities for the slightly more polar protein interior.

Direct relations between individual amino acid hydrophobicities<sup>1</sup> and the structure and stabilities of soluble proteins have been established (Yutani *et al.*, 1984; Matsumura *et al.*, 1988; Kellis *et al.*, 1989; Shortle *et al.*, 1990; O'Neill & DeGrado, 1990; Blaber *et al.*, 1993; Jackson *et al.*, 1993). A similar role of amino acid hydrophobicities in the determination of the topology of membrane proteins has been postulated (von Heijne, 1979, 1981; Engelman *et al.*, 1986). Hydropathy plots are based on this idea and have proven to be an indispensable tool in the analysis of membrane protein structure.

Numerous hydrophobicity or polarity scales for amino acids have been developed [for a listing of 82 sets of hydrophobic indices, see Nakai *et al.* (1988)]. Most indices are based on various physical properties of small peptides and side chain analogs and on the distribution of amino acids

in proteins and membranes. The hydropathy scale of Kyte and Doolittle (1982) is most widely used. However, scales specifically designed to identify transmembrane helices exist (Engelman *et al.*, 1986). Despite the extensive use of hydropathy plots to evaluate and predict the structure of membrane proteins, this approach has yet to be experimentally validated with respect to membranes, and there is ongoing discussion regarding which hydropathy indices are most relevant for membrane proteins (Crimi & Degli Eposti, 1991).

The aim of this work was to measure directly and quantitatively the membrane affinities of individual amino acids by examination of the partitioning into lipid bilayers of a membrane-interacting polypeptide host containing single amino acid substitutions at a guest site. While the membrane environment can easily be mimicked using synthetic phospholipid vesicles, the bilayer environment itself is unique in ways that severely restrict the choice of the host polypeptide. Amino acid derivatives have proven very useful for solvent transfer studies (Nozaki & Tanford, 1971; Fauchere & Pliska, 1983), but for very small peptides, the binding topology, and particularly the location of the guest site in the membrane, may depend strongly on the amino acid composition. Tripeptides, for example, yield values much lower than expected from the classical hydrophobic effect (Jacobs & White, 1989). In contrast, a large membrane protein is not a suitable host, since it will be permanently and irreversibly inserted into membranes. Peptides of intermediate size (10–30 aa)<sup>2</sup> such as membrane-interacting N-terminal leader sequences present a compromise between these extremes and are easy to synthesize and purify. In this study, we use a host based on the 25-residue leader sequence of yeast cytochrome *c* oxidase. We synthesized 14 different peptides,

<sup>†</sup> This work was supported by the startup fund from the University of California, Berkeley, NIH Grant GM51290-01, and ACS PRF Grant 28160-G7. Y.-K. S. is a 1995 Searle Scholar.

<sup>\*</sup> To whom correspondence should be addressed.

<sup>‡</sup> Department of Chemistry.

<sup>§</sup> Howard Hughes Medical Institute and Department of Molecular and Cell Biology.

<sup>®</sup> Abstract published in *Advance ACS Abstracts*, January 15, 1996.

<sup>1</sup> Although the term “hydrophobic” can be defined in several ways, the hydrophobicity of an amino acid side chain is most conveniently defined as the free energy of transfer from organic solvents to water at room temperature (Dill, 1990). This purely experimental definition does not involve a detailed microscopic interpretation and can easily be extended to include a rather unusual temperature dependence, due to a large reduction of heat capacity associated with the removal of a nonpolar solute from water (Baldwin, 1986).

<sup>2</sup> Abbreviations: aa, amino acid; CD, circular dichroism; COX IV, cytochrome *c* oxidase subunit IV; EDDA, ethylenediamine-*N,N'*-diacetic acid; EPR, electron paramagnetic resonance; HPLC, high-performance liquid chromatography; IACSL, 3-(2-iodoacetamido)-PROXYL spin-label; MOPS, 3-(*N*-morpholino)propanesulfonic acid; MTSSL, *S*-[(1-oxy-2,2,5,5-tetramethylpyrrolin-3-yl)methyl]methanethiosulfonate spin-label; PC, phosphatidylcholine; POPC, 1-palmitoyl-2-oleoylphosphatidylcholine; POPG, 1-palmitoyl-2-oleoylphosphatidylglycerol.

each containing a different uncharged amino acid at a single guest site, and used electron paramagnetic resonance to examine their partitioning into phospholipid bilayers. The membrane affinities are directly obtained as free energy differences ( $\Delta\Delta G_{\text{bilayer}}$ ). The  $\Delta\Delta G_{\text{bilayer}}$  values equal hydrophobicities assessed from 1-octanol–water partitioning of *N*-acetyl amino acid amides (Fauchere & Pliska, 1983; Eisenberg & McLachlan, 1986) and quantitatively establish the contribution of individual amino acids to protein–membrane interactions.

## MATERIALS AND METHODS

**Materials.** Resin and Fmoc-protected amino acids for peptide synthesis were obtained from Nova Biochem (La Jolla, CA) and Bachem California (Torrance, CA), respectively. Phospholipids (POPC and POPG) were from Avanti Polar Lipids (Birmingham, AL). Buffer A [2 mM MOPS, 0.2 mM ethylenediaminetetraacetic acid (EDTA), and 5 mM  $\text{NH}_4\text{OAc}$ , adjusted to pH 7.2 with NaOH] was prepared using reagents from Sigma Chemical Co. (St. Louis, MO). 4-Carboxy-TEMPO and IACSL were purchased from Aldrich Chemical Co. (Milwaukee, WI), and MTSSL was obtained from Reanal (Hungary). Ni-EDDA was a gift from Prof. W. L. Hubbell at the Jules Stein Eye Institute at the UCLA School of Medicine.

**Peptide Synthesis, Spin-Labeling, and Purification.** The peptides were made by solid phase peptide synthesis using (9-fluorenylmethoxy)carbonyl (Fmoc) amino acids and an automated peptide synthesizer (Applied Biosystems 430A, Emeryville, CA). The peptides were purified by reversed phase HPLC on a Vydac  $\text{C}_{18}$  column (The Separations Group, Hesperia, CA) as described previously (Yu *et al.*, 1994) and lyophilized. For spin-labeling, the peptides were dissolved in 10 mM MOPS buffer (pH 7.0) and reacted with an approximately 2-fold molar excess of MTSSL at room temperature for 1 h. Following purification by reversed-phase HPLC, the spin-labeled peptides were lyophilized and stored dry at  $-20^\circ\text{C}$ . The identities and purities of the spin-labeled peptides were assessed by electrospray-ionization mass spectrometry (Hewlett-Packard 5989A); all molecular masses were within 0.5 amu of theoretical values (purities > 96%).

**Circular Dichroism Spectroscopy.** CD spectra of peptides in solution (10  $\mu\text{M}$  peptide, 20 mM  $\text{PO}_4$  buffer, pH 7.2, and  $20^\circ\text{C}$ ) were measured in a 1 cm cell using a Jasco J-600 spectrometer.

**Preparation of Phospholipid Vesicles.** POPC and POPG were mixed in chloroform, and  $\text{CHCl}_3$  was removed by a stream of nitrogen. The dry lipid was then placed under vacuum for several hours to remove residual  $\text{CHCl}_3$  and dissolved in buffer A to yield a total lipid concentration of 65 mM. Unilamellar vesicles were prepared by extrusion through 100 nm pore size polycarbonate membranes in a LiposoFast miniextruder (Avestine, Canada) following five cycles of freeze–thaw.

**EPR Spectroscopy.** EPR spectra of peptides in solution and when mixed with phospholipid vesicles were performed using a Bruker ESP300 spectrometer equipped with a loop gap resonator (Medical Advances Inc., Milwaukee, WI) and a low-noise amplifier (Miteq, Hauppauge, NY). Immediately before measurements, spin-labeled peptides were dissolved in buffer A to the desired concentration and introduced into

previously prepared suspensions of phospholipid vesicles, and the resulting solution was thoroughly mixed by vortexing and allowed to stand for  $1/2$  h before EPR measurements were performed at  $21^\circ\text{C}$ .

**Immersion Depth Measurements.** The immersion depths of the nitroxide spin-labels were measured by the EPR collision gradient method developed by Altenbach *et al.* (1994). The depth measurements were performed using solutions of peptide bound to POPC vesicles with 10 mol % POPG placed in a gas-permeable TPX capillary to allow saturation of the samples with air or nitrogen. Under these conditions, over 98% of the peptide is bound to the vesicles. The EPR spectra at 0.1, 0.25, 1, 4, 8, 10, 16, 25, and 40 mW incident microwave power were measured, and the peak-to-peak amplitudes of the first-derivative  $M_1 = 0$  EPR lines were used to obtain the saturation profiles in the presence of membrane-permeable ( $\text{O}_2$ ) and -impermeable (Ni-EDDA) paramagnetic relaxants. The measurements were performed and analyzed using a calibration curve based on measurements of spin-labeled bacteriorhodopsins as described previously (Yu *et al.*, 1994).

## RESULTS

**The Host–Guest System.** The host–guest system needs to fulfill several criteria to be suitable for direct measurements of membrane affinities of individual amino acids. Most importantly, the host should insert into the lipid bilayer with the guest site completely buried in the bilayer upon binding. Ideally, the binding should be reversible to allow quantitative measurements of the partition equilibrium. Furthermore, the guest site should also be completely exposed to water in the unbound state, and substitutions at the guest site should not significantly affect the structure of the peptide in solution or that of the peptide–membrane complex. If changes in the partition constant are to truly reflect the membrane affinities of individual amino acids, it is also required that neither the secondary structure propensity of the guest aa nor interactions between the guest aa and its nearest neighbors significantly contribute to the free energy of binding.

The host used here, derived from the amphipathic presequence of subunit IV of yeast cytochrome *c* oxidase (COX IV), binds reversibly to phospholipid bilayers as a monomer with the topology depicted in Figure 1. This topological model is based on the results of measurements of the immersion depth of spin-labels attached to various sites near the  $\text{NH}_2$  terminal end of the bilayer-bound presequence, as well as on studies of the electrostatic contribution to the binding and energetic considerations (Yu *et al.*, 1994; Thorgeirsson *et al.*, 1995).

The amino acid sequence of the host is  $\text{H}_2\text{N-Met-Leu-Ser-Cys-Arg-Gln-X-Ile-Arg-Phe-Phe-Lys-Pro-Ala-Thr-Arg-Thr-Leu-Ser-Ser-Ser-Arg-Tyr-Leu-Leu-COOH}$ . The guest site (X) is at position 7, midway between the Arg5 and Arg9 residues in the  $\text{NH}_2$  terminal region. We introduced 14 different amino acids at the guest site to measure membrane affinities. We excluded Glu, Asp, His, Lys, and Arg in this study because introduction of charged residues would alter the binding topology (Yu *et al.*, 1994; Thorgeirsson *et al.*, 1995). The host contains a single cysteine residue at position 4 to allow nitroxide spin-labeling for electron paramagnetic resonance (EPR) measurements of the binding equilibria. The EPR spectrum for the nitroxide spin-label is very sensitive

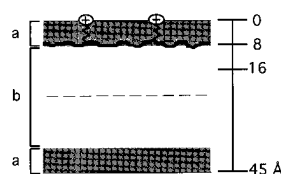


FIGURE 1: Schematic drawing showing the binding topology of the COX IV peptide in phospholipid bilayers at low surface charge. The center of the bilayer is indicated by a dashed line, and the head group regions (a) are indicated by the shaded areas between the acyl chain region (b) and the water phase. The scale on the right shows distance in angstroms, from the bilayer surface (Wiener & White, 1992). The position of the extended peptide backbone is represented by a line at the interface of the head group and acyl chain regions of the bilayer. Two representative arginine side chains are shown extending from the backbone toward the surface of the bilayer such that the hydrocarbon arm is buried in the bilayer while the charges remain near the surface of the bilayer. This model is based on our previous measurements of the immersion depths of spin-labels attached to various positions near the  $\text{NH}_2$  terminal end of the peptide showing that the backbone is buried about 8 Å below the surface of the bilayer (Yu *et al.*, 1994), our studies of the electrostatics of bilayer binding (Thorgeirsson *et al.*, 1995), and energetic considerations (see Text).

to the viscosity of the surroundings, and the lines in the EPR spectrum of a nitroxide spin-label attached to a bilayer-bound peptide are substantially broader than those of the typical fast motional spectrum of a nitroxide spin-label attached to a peptide in solution. The proximity of the spin-label to the guest site allows the monitoring of changes in the position of the peptide backbone near the guest site using the collision gradient method.

*The Host Has an Extended Structure in Solution and in the Bilayer.* Previous CD studies of the wild-type sequence in solution and in lipid bilayers (Tamm & Bartholdus, 1990; Roise *et al.*, 1986) show that the sequence has an extended, nonhelical conformation both in solution and in phospholipid bilayers containing less than 20% negatively charged lipid. Analysis of EPR spectra for a series of COX IV peptides containing two spin-labels in the  $\text{NH}_2$  terminal region shows that this region has an extended structure in solution and in lipid vesicles with a low surface charge (Yu *et al.*, 1994).

It is interesting that the sequence does not bind as a helix to bilayers with low surface charge, since it is highly amphipathic. However, upon helix formation, the five positive charges are expected to line up on one face of the helix, and electrostatic repulsion between the positive charges could act as a strong force opposing helix formation. The presence of negatively charged lipid might stabilize helix formation by reducing this repulsion, and in the presence of vesicles containing more than 20% negatively charged lipid, helical conformations are detected by CD spectroscopy (Tamm & Bartholdus, 1990). In addition to stabilizing helical conformations, the negatively charged lipid head groups produce an electrostatic component to the binding energy ( $\Delta G^{\text{el}} = zF\Psi$ ). The binding energetics is completely dominated by the electrostatic component under conditions that promote the formation of helical conformations, and the host binds too strongly to allow quantitative EPR measurements (Thorgeirsson *et al.*, 1995).

*Guest Residues Do Not Induce Secondary Structure.* CD spectra of the peptides indicate that in solution they are all in an extended conformation, containing little or no  $\alpha$ -helix, and that the substitutions induce no significant changes in secondary structure (Figure 2). Neither the incorporation

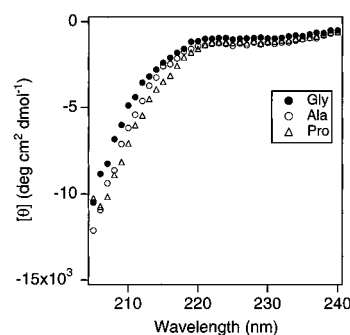


FIGURE 2: CD spectra for peptides containing Gly, Ala, and Pro residues at the guest site (12  $\mu\text{M}$  peptide, 20 mM  $\text{PO}_4$  buffer, pH 7.2, and 20  $^\circ\text{C}$ ). The spectra agree well with previous CD measurements for the wild-type signal sequence in solution, which suggested that the secondary structure is extended or mainly random coil (Tamm & Bartholdus, 1990; Roise *et al.*, 1986). The peptides contain little or no  $\alpha$ -helix. The average value of  $\Theta_{222}$  is  $-1850 (\pm 550)$   $\text{deg cm}^2 \text{dmol}^{-1}$  for all of the peptides studied. A value near  $-25\,000 \text{ deg cm}^2 \text{dmol}^{-1}$  is expected for a completely helical peptide of this size. Ala has a high  $\alpha$ -helix propensity, whereas Gly and Pro are helix-destabilizing (Blaber *et al.*, 1993; O'Neill & DeGrado, 1990). The CD spectra for the peptides containing these residues at the guest site are all similar to that of the wild type (Tamm & Bartholdus, 1990), indicating that neither the incorporation of the spin-label at position 4 nor the amino acid substitutions at the guest site cause significant alterations in secondary structure.

of the spin-label nor the amino acid substitutions lead to any alteration in secondary structure as CD spectra for all the peptides in solution agree well with that for the wild-type signal sequence. We also observe no changes in the EPR line shape for bilayer-bound peptides containing the amino acid substitutions. As the EPR line shape is very sensitive to changes in the mobility of the spin-label, this indicates that the structure of the peptide in the bilayer is not affected and that the peptides containing the various guest residues maintain an extended structure.

*The Guest Site Is Immersed in the Bilayer.* Spin-labels attached to cysteines placed at positions 3–8 and 19 in the presequence were immersed at depths between 13 and 16 Å below the bilayer surface (Yu *et al.*, 1994). This depth corresponds to a location between the fifth and seventh carbon on the acyl chains of the lipid. This depth, however, does not necessarily reflect the position of the peptide backbone since the spin-labeled cysteine side chain is fairly apolar and may preferentially orient toward the bilayer interior. The effective “arm length” of the spin-labeled cysteine side chain is  $\sim 6$  Å (Rabenstein & Shin, 1995), and the backbone is thus located somewhere between 7 and 22 Å below the surface. Considering the high cost of burying an incompletely hydrogen-bonded peptide in the acyl chain region and the cost of burying the charged ends of the arginine and lysine side chains in a low dielectric environment, it is unlikely that the extended backbone is buried deep in the acyl chain region. Combining the experimental results and energetic considerations, we conclude that the backbone is located approximately 8 Å below the surface, with the lysine and four arginine side chains extending from the backbone toward the surface of the bilayer (Figure 1).

The depth of immersion of the spin-label at position 4 was determined for all the peptides using the collision gradient method (Altenbach *et al.*, 1994; Yu *et al.*, 1994). For all the peptides, we find that the nitroxide spin-labels are buried in the acyl chain region at an average depth of 16

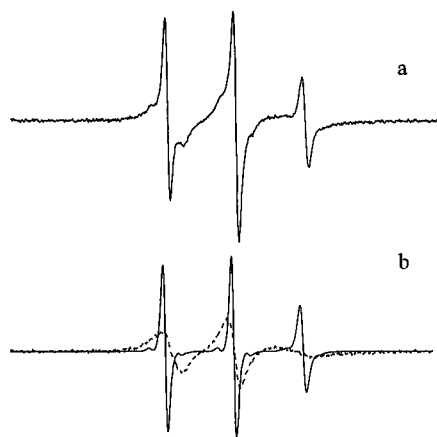


FIGURE 3: (a) EPR spectrum for the peptide containing Val at the guest site in the presence of 1-palmitoyl-2-oleoylphosphatidylcholine (POPC) lipid vesicles containing 2.4 mol % 1-palmitoyl-2-oleoylphosphatidylglycerol (POPG) (2 mM MOPS, pH 7.2, 105 mM  $\text{NH}_4\text{OAc}$ , 6 mM NaCl, and 0.2 mM EDTA). The total peptide concentration is 77  $\mu\text{M}$ , and the lipid concentration is 39 mM. (b) The broad spectrum for the membrane-bound peptide (---) remains after subtraction of the sharp solution spectrum (—) from the composite spectrum in a. The scan width is 100 G. The concentrations of the membrane-bound and free peptides are spectral integrations in reference to 100  $\mu\text{M}$  TEMPO standards.

Table 1:  $\Delta\Delta G$  Values for Bilayer-to-Water, and Alcohol-to-Water Transfer

guest amino acid	$\Delta\Delta G_{\text{bilayer}}$ (kcal/mol)	$\Delta\Delta G_{\text{octanol}}^a$ (kcal/mol)	$\Delta\Delta G_{\text{ethanol}}^b$ (kcal/mol)
Trp	$2.46 \pm 0.15$	3.07	3.2
Leu	$2.41 \pm 0.15$	2.32	
Phe	$2.40 \pm 0.15$	2.44	2.6
Ile	$2.36 \pm 0.15$	2.46	
Val	$1.72 \pm 0.15$	1.66	1.47
Met	$1.68 \pm 0.15$	1.68	1.3
Tyr	$1.11 \pm 0.15$	1.31	2.4
Ala	$0.64 \pm 0.15$	0.42	0.52
Thr	$0.05 \pm 0.15$	0.35	0.4
Gly	0	0	0
Ser	$-0.25 \pm 0.15$	0.05	-0.3
Gln	$-0.26 \pm 0.30^c$	-0.30	-0.26
Asn	$-0.64 \pm 0.30^c$	-0.82	-0.15
Pro	$-0.76 \pm 0.15$	0.98	

<sup>a</sup> Fauchere and Pliska (1983) and Eisenberg and McLachlan (1986).

<sup>b</sup> Nozaki and Tanford (1971). <sup>c</sup> Values for Gln and Asn were determined in comparison with values for Ser using peptides containing Gln, Asn, or Ser at position 7 in a host containing an additional substitution from Ser to Phe at position 3 to increase the extent of binding.

Å ( $\sigma = 1.9$  Å), which is a depth corresponding to that of the seventh carbon on the acyl chain of the lipid molecule. The extended structure in solution ensures that the guest side is fully exposed to water in solution, and since the amino acid substitutions do not significantly affect the position of the peptide backbone, the amino acid side chains are completely removed from the water phase upon membrane binding.

**Membrane Affinities ( $\Delta\Delta G_{\text{bilayer}}$ ).** The transfer free energies,  $\Delta\Delta G_{\text{bilayer}}$  (relative to glycine), obtained from analysis of equilibrium partition constants which are determined using EPR spectral subtraction (Figure 3), are listed in Table 1. The transfer energies were calculated using a simple partition model described previously (Thorgeirsson *et al.*, 1995). Briefly,  $r = C_b/C_f = {}^5/9 KC_L \exp(-zF\Psi/RT)$ , where  $C_L$ ,  $C_b$ , and  $C_f$  are the concentrations of lipid, bound, and free peptide, respectively,  $z$  is the peptide charge,  $F$  is Faraday's

constant, and  $\Psi$  is the Gouy–Chapman–Stern surface potential. The surface potential of the lipid bilayers was controlled by varying the amount of negatively charged lipid and the concentration of the membrane-permeable electrolyte  $\text{NH}_4\text{OAc}$ . The EPR measurements yield the ratios  $r_i$ , and for any two peptides at the same lipid concentration,  $\Delta\Delta G = -RT \ln (r_1/r_2) - \Delta\Delta G^{\text{el}}$ . The electrostatic term,  $\Delta\Delta G^{\text{el}} = zF(\Psi_1 - \Psi_2)$ , only contributes when surface potentials differ but is not always negligible in vesicles of identical composition because peptide binding reduces the surface charge. Measurements were conducted at various surface potentials (1–4% negatively charged lipid, 80–150 mM salt) and peptide concentrations varied to optimize conditions ( $r$  near unity,  $|\Delta\Delta G^{\text{el}}| < 0.1$  kcal/mol). From 70 measurements ( $\sim 5$  for each peptide), we obtained 48 difference values representing 48 equations with 13 unknowns. We calculated the 13 overdetermined  $\Delta\Delta G$  values using a least squares method, and the experimental difference values are recovered with a standard deviation of 0.15 kcal/mol using the optimized  $\Delta\Delta G$  values in Table 1. The hydrophobicities of amino acid side chains assessed from alcohol–water partitioning data (Fauchere & Pliska, 1983; Eisenberg & McLachlan, 1986; Nozaki & Tanford, 1971) are also listed in Table 1, and there is a strong correlation between  $\Delta\Delta G_{\text{bilayer}}$  and individual residue hydrophobicities (Figure 4a).

## DISCUSSION

Deber and Li (1995) discuss four primary equilibria that may occur upon the partitioning of amphipathic peptides into membranes: (1) helix–coil transition in the aqueous phase, (2) transfer of helical peptides between the aqueous and membrane phases, (3) helix–coil equilibria within the membrane, and (4) partitioning of random coil peptides into the membrane. The energetics of membrane partitioning will depend upon which of these processes take place, and each system has to be evaluated with regard to the individual contributions to the free energy of transfer.

Here we use conditions under which the COX IV peptide partitions into the lipid bilayer in an extended conformation. By using conditions that do not promote helical conformations, the partitioning involves a single predictable mode of interaction and the energetics of helix formation do not contribute to the free energy of transfer. As discussed by Deber and Li (1995), it is desirable that the membrane insertion occurs in a single mode (either process 2 or 4 above) without the involvement of the helix–coil equilibria (processes 1 and 3 above).

Using a host peptide inserting as an amphipathic helix into the membrane might appear to be advantageous for the experiment. The rigidity of the  $\alpha$ -helical structure and the consistency of the heptad repeat would ensure that the side chains of guest residues located on the hydrophobic face of the  $\alpha$ -helix would be well-buried and directed toward the interior of the bilayer. However, many peptides that form amphipathic helices upon membrane binding have a random structure in solution. In this case, the energetics of helix formation must contribute to the stability of the membrane–polypeptide complex. Thus, differences in the binding of peptides containing different guest residues most likely would present some combination of the bilayer affinities and the helical propensities of individual amino acids. This effect

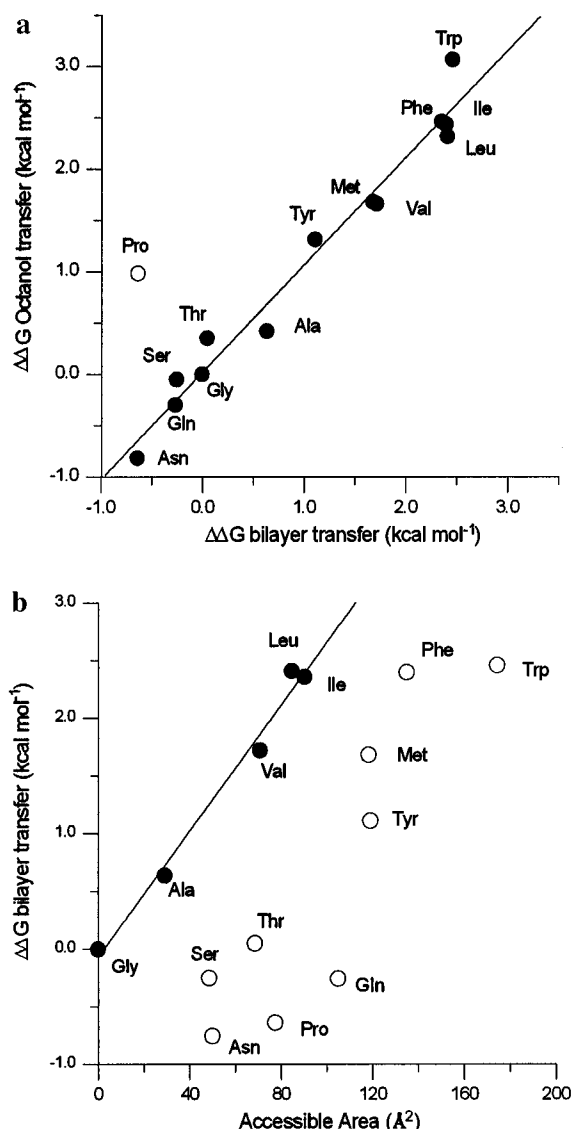


FIGURE 4: (a) Free energies of transfer from bilayer to water ( $\Delta\Delta G$  relative to Gly) plotted against the octanol–water transfer free energies (Fauchere & Pliska, 1983; Eisenberg & McLachlan, 1986). The straight line represents the best fit to the data with a slope of 1.04 ( $R = 0.98$ ) excluding proline. (b)  $\Delta\Delta G_{\text{bilayer}}$  as a function of water accessible surface areas calculated using the accessibilities for Ala-X-Ala in an extended conformation (Lee & Richards, 1971) and subtracting the area for Gly from all values. Areas for Gln and Asn are obtained from the stochastic areas for Gln, Asn, and Gly in Gly-X-Gly (Rose *et al.*, 1985). The best fit of the points for the aliphatic side chains has a slope of 27  $\text{cal mol}^{-1} \text{\AA}^{-2}$  ( $R = 0.99$ ).

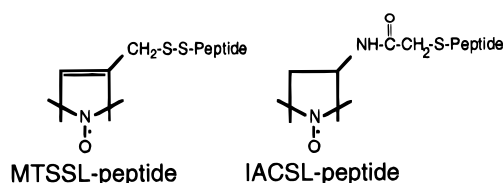
could significantly affect the outcome as helical propensities range up to  $\sim 1$  kcal/mol (Deber & Li, 1995; O'Neill & DeGrado, 1990; Blaber *et al.*, 1993). Introduction of guest residues with very low helical propensities (helix breakers) might also change the structure of the membrane-associated form. Interactions between the guest aa and its nearest neighbors in the helix may also lead to context dependent results. When the host also forms amphiphilic  $\alpha$ -helices in the aqueous phase, it is often due to the formation of multimers or aggregates. This is disadvantageous as the introduction of a guest amino acid might affect the stability of the multimers, complicating the analysis of the results.

The COX IV presequence is almost an ideal host for measurement the membrane affinities of individual amino acids. A central feature of the binding topology is that the peptide backbone is buried at least 7  $\text{\AA}$  below the surface of

the lipid bilayer in an extended structure (Figure 1), such that the side chains of the guest residues are buried within the bilayer, in either the head group region or the acyl chain region. The extended structure of the peptide ensures complete exposure to the water and lipid phases in the unbound and bound states, respectively. CD measurements show that the substitutions do not significantly affect the structure of the host in solution (Figure 2). The structural differences between membrane–peptide complexes containing different guest residues are likely to be limited to changes in the orientation of the guest residue within the bilayer, since the position of the backbone is fixed near the beginning of the acyl chain region and each side chain is free to find its preferred orientation within the membrane. This conclusion is supported by the small variance in the immersion depth of spin-labels attached to various positions near the N-terminus of the peptide and the invariance of the immersion depth of the spin-label attached to peptides containing different substitutions at the guest site. Furthermore, the extended conformation will tend to minimize any context dependence since direct interactions between the guest and its nearest neighbors are less important than in a more compact structure.

As a consequence of the extended structure in the bilayer, the guest residue has freedom to orient within the bilayer. While hydrophobic amino acids at the guest site are likely to be buried in the acyl chain region, just as is the case for the hydrophobic MTSSL-modified cysteine side chain, the more polar side chains may be located in the head group region of the bilayer.

To assess the effect of the polarity of the residue at the guest site on its position in the bilayer, we used a peptide containing Leu at position 4 and Cys at position 7 and labeled the peptide with two different spin-labels, MTSSL and IACSL. The modified cysteine side chains have very



different polarities, and since their immersion depth can be directly assessed using the collision gradient method, the peptides provide a good control for the effect of side chain polarity on location within the bilayer. The cysteine side chain modified with MTSSL has a membrane affinity similar to that of Trp (Yu *et al.*, 1994). By comparing the partition equilibria for the two peptides, we find that the IAC-modified Cys side chain has a membrane affinity that is about 2.5 kcal/mol lower than that for the MTSSL-modified Cys side chain. The immersion depth was measured using the collision gradient method, and the IAC spin-label is located  $\sim 10$   $\text{\AA}$  below the bilayer surface. Although it is buried less deeply than MTSSL (14  $\text{\AA}$ ), the IAC spin-label is still located in the acyl chain region despite the much lower membrane affinity. The solvent-sensitive hyperfine-coupling constants ( $A_N$ ), obtained by measuring the peak-to-peak distances in the EPR spectra, are also consistent with a location in the acyl chain region for both spin-labels. The values are 16.1 G (water)/14.8 G (membrane-bound) for MTSSL and 15.8 G (water)/14.8 G (membrane-bound) for IAC.

Figure 4a shows that  $\Delta\Delta G_{\text{bilayer}}$  values equal the hydrophobicities assessed from alcohol–water transfer studies. This result has two important implications. First, the effect of the substitution at one site on the overall stability of the peptide in the bilayer is almost exclusively accounted for by the change in hydrophobicity. Second, the classical viewpoint that the hydrophobic effect is mainly due to the free energy of removal of the solute from water also holds for membrane insertion. Thus, the energy cost of creating the cavity in the membrane and specific interactions between amino acid side chains and the phospholipid are unimportant.

A previous study of the bilayer binding of hydrophobic tripeptides of the form Ala-X-Ala-*O*-*tert*-butyl (X = Gly, Ala, Leu, Phe, or Trp) gave much smaller  $\Delta\Delta G$  values, most likely due to incomplete burial of the substitution site in the bilayer (Jacobs & White, 1989; White & Wimley, 1994). For small peptides, the depth of immersion in a lipid bilayer is likely to be strongly dependent on the amino acid composition. Using neutron diffraction, Jacobs and White (1989) determined the distribution in the bilayer for a tripeptide containing Trp at the central position and found that only 13% of the bilayer-bound population was located inside the hydrocarbon core of the bilayer.

Correlations have been reported between water accessible areas (Lee & Richards, 1971) of amino acid side chains and hydrophobic energies. This relationship was investigated for  $\Delta\Delta G_{\text{bilayer}}$  (Figure 4b). For the aliphatic side chains G, A, V, L, and I, the relationship is linear with a slope of 27 cal  $\text{\AA}^{-2} \text{mol}^{-1}$  ( $R = 0.99$ ). The slope is within the range of generally accepted values for the hydrophobic effect which is 16–31 cal  $\text{mol}^{-1} \text{\AA}^{-2}$  (Eisenberg & McLachlan, 1986; Reynolds *et al.*, 1974; Chothia, 1974; Hermann, 1974). The membrane affinities of the polar side chains are lowered due to specific interactions with water. Interestingly, the membrane affinity of Phe is significantly lower than might be expected from surface area considerations alone (Figure 4b). Although the aromatic side chains are generally considered very hydrophobic, the aromatic  $\Pi$ -system can hydrogen bond to water (Suzuki *et al.*, 1993) which might lower the bilayer affinity from that expected for an aliphatic side chain with a similar surface area. In the case of Trp and Tyr, such effects need to be considered together with the polarity or hydrogen-bonding character of the hydroxyl and amino groups.

The  $\Delta\Delta G$  values obtained here for the more hydrophobic residues most likely reflect the affinities of individual amino acids for the acyl chain region. In the case of the more polar residues, the  $\Delta\Delta G$  values may represent the free energy of transfer from the head group region rather than the hydrocarbon core. Regardless of their position in the bilayer, residues capable of forming hydrogen bonds would prefer to remain hydrogen-bonded upon transfer into the bilayer. The side chains may be able to form hydrogen bonds with water present in the head group region, with water molecules accompanying them into the acyl chain region of the bilayer, or to the carbonyl groups of the lipid. In fact, the results of Jacobs and White (1989) on the distribution profiles for water and Ala-Trp-Ala-*O*-*tert*-butyl peptide in DOPC bilayers clearly show a large increase in the penetration of water into the bilayer, with the resulting water distribution in the bilayer mirroring that of the peptide (Jacobs & White, 1989).

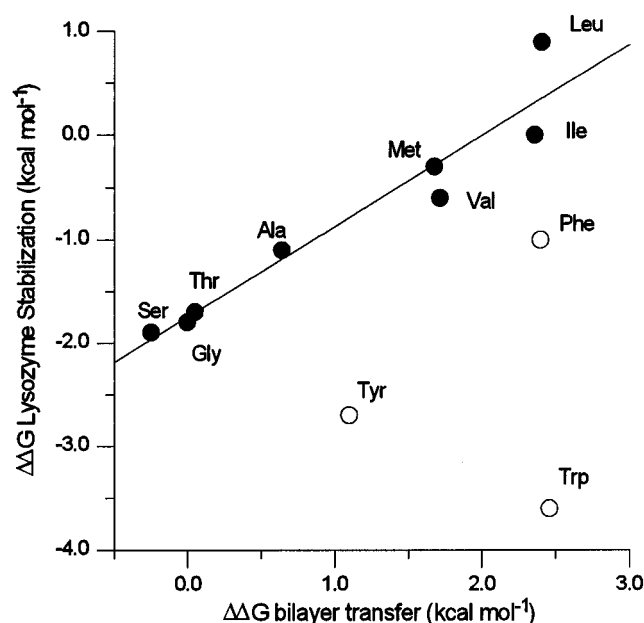


FIGURE 5: Free energy of stabilization for T4 lysozyme ( $\Delta\Delta G_{\text{lysozyme}}$ ) vs  $\Delta\Delta G_{\text{bilayer}}$ . Protein free energies are obtained from the thermal stabilities of mutant T4 lysozymes containing single replacements at position 3 relative to Ile at pH 2.0 [from Matsumura *et al.* (1988)]. The straight line (slope = 0.87 and  $R = 0.96$ ) is the best fit to the data omitting Tyr, Phe, and Trp, for which crystallographic analysis showed altered structure (Matsumura *et al.*, 1988). A slope of 0.87 is consistent with the approximately 20% solvent accessibility at position 3 in T4 lysozyme. However, the effect of internal substitutions on protein stability may vary from site to site, and studies involving the truncation of internal aliphatic side chains yield higher values (Jackson *et al.*, 1993).

Bilayer-exposed residues are on the average more hydrophobic than interior residues in membrane proteins, whereas the average hydrophobicity of the interior is similar to that of the interior of water-soluble proteins (Rees *et al.*, 1989). It is therefore of interest to compare  $\Delta\Delta G_{\text{bilayer}}$  values to estimates of the free energy associated with burying individual amino acids in the protein interior. Matsumura *et al.* (1988) investigated changes in the thermal stability of T4 lysozyme upon amino acid replacements of Ile3 which is buried near the surface of the protein and about 80% solvent inaccessible. The results on T4 lysozyme correlate strongly with  $\Delta\Delta G_{\text{bilayer}}$  with a slope of 0.87 (Figure 5). However, several other studies have given significantly higher  $\Delta\Delta G$  values than this study of T4 lysozyme (Kellis *et al.*, 1989; Shortle *et al.*, 1990; Jackson *et al.*, 1993), and further experimental and theoretical work is required to better understand the relationship between the hydrophobicities of internal residues and protein stability (Dill, 1990; Honig & Yang, 1995).

**Conclusions.** The  $\Delta\Delta G_{\text{bilayer}}$  values reported here are based on the partitioning of peptides in an extended conformation into phospholipid bilayers and represent a measurement of the membrane affinities of uncharged amino acids without contributions from the intrinsic secondary structure propensities of individual amino acids. The affinities of uncharged amino acids for the lipid bilayer ( $\Delta\Delta G_{\text{bilayer}}$ ) equal the free energy of their transfer from 1-octanol to water ( $\Delta\Delta G_{\text{transfer}}$ ). The membrane affinities are simply represented by the free energy gained from removal of the amino acid side chains from water. In this aspect, the role of the hydrophobic effect in bilayer partition-

ing is thus similar to its role in the folding of globular proteins, and the  $\Delta\Delta G_{\text{bilayer}}$  values correlate well with previous measurements of the free energy of transfer of amino acids into the interior of soluble proteins (Matsumura *et al.*, 1988).

## ACKNOWLEDGMENT

We thank Lewis Hou and Thai Nguyen for work on synthesis and purification of peptides, Dr. Ignacio Tinoco, Jr., for the use of his circular dichroism spectrophotometer, and Drs. Wayne L. Hubbell and Christian Altenbach for sending us Ni-EDDA and bacteriorhodopsin depth calibration data.

## REFERENCES

- Altenbach, C., Greenhalgh, D. A., Khorana, H. G., & Hubbell, W. L. (1994) *Proc. Natl. Acad. Sci. U.S.A.* 91, 1667–1671.
- Baldwin, R. L. (1986) *Proc. Natl. Acad. Sci. U.S.A.* 83, 8069–8072.
- Blaber, M., Zhang, X.-J., & Matthews, B. W. (1993) *Science* 260, 1637–1640.
- Chothia, C. (1974) *Nature* 248, 338–339.
- Crimi, M., & Degli Eposti, M. (1991) *Trends Biochem. Sci.* 16, 119.
- Deber, C. M., & Li, S.-C. (1995) *Biopolymers* 37, 295–318.
- Diesenhofer, J., Epp, O., Miki, K., Huber, R., & Michel, H. (1985) *Nature* 318, 618–624.
- Dill, K. A. (1990) *Biochemistry* 29, 7133–7155.
- Eisenberg, D., & McLachlan, A. (1986) *Nature* 319, 199–203.
- Engelman, D. M., & Zacchaj, G. (1980) *Proc. Natl. Acad. Sci. U.S.A.* 77, 5894–5898.
- Engelman, D. M., Steitz, T. A., & Goldman, A. (1986) *Annu. Rev. Biophys. Biophys. Chem.* 15, 321–353.
- Fauchere, J.-L., & Pliska, V. (1983) *Eur. J. Med. Chem.* 18, 369–375.
- Hermann, R. B. (1971) *Proc. Natl. Acad. Sci. U.S.A.* 74, 4144–4145.
- Honig, B., & Yang, A.-S. (1995) *Adv. Protein Chem.* 46, 27–57.
- Jackson, S. E., Moracci, M., elMasry, N., Johnson, C. M., & Fersht, A. R. (1993) *Biochemistry* 32, 11259–11269.
- Jacobs, R. E., & White, S. H. (1989) *Biochemistry* 28, 3421–3437.
- Kauzmann, W. (1959) *Adv. Protein Chem.* 14, 1–63.
- Kellis, J. T., Nyberg, K., & Fersht, A. R. (1989) *Biochemistry* 28, 4914–4922.
- Kyte, J., & Doolittle, R. F. (1982) *J. Mol. Biol.* 157, 105–132.
- Lee, B., & Richards, F. M. (1971) *J. Mol. Biol.* 55, 379–400.
- Matsumura, M., Becktel, W. J., & Matthews, B. W. (1988) *Nature* 334, 406–410.
- Nakai, K., Kidera, A., & Kanehisa, M. (1988) *Protein Eng.* 2, 93.
- Nozaki, Y., & Tanford, C. (1971) *J. Biol. Chem.* 246, 2211–2217.
- O'Neill, K. T., & DeGrado, W. F. (1990) *Science* 250, 646–651.
- Rabenstein, M. D., & Shin, Y.-K. (1995) *Proc. Natl. Acad. Sci. U.S.A.* 92, 8239–8243.
- Rees, D. C., DeAntonio, L., & Eisenberg, D. (1989) *Science* 245, 510–513.
- Reynolds, J. A., Gilbert, D. B., & Tanford, C. (1974) *Proc. Natl. Acad. Sci. U.S.A.* 71, 2925–2927.
- Roise, D., Tomich, S. J., Richards, J. M., & Schatz, G. (1986) *EMBO J.* 5, 1327–1334.
- Rose, G. D., Geselowitz, A. R., Lesser, G. J., Lee, R. H., & Zehfus, M. H. (1985) *Science* 229, 834–838.
- Shortle, D., Stites, W. E., & Meeker, A. K. (1990) *Biochemistry* 29, 8033–8041.
- Suzuki, S., Green, P. G., Bumgarner, R. E., Dasgupta, S., Goddard, W. A., & Blake, G. A. (1993) *Science* 257, 942–945.
- Tamm, L. K., & Bartholdus, I. (1990) *FEBS Lett.* 272, 29–33.
- Thorgeirsson, T. E., Yu, Y. G., & Shin, Y.-K. (1995) *Biochemistry* 34, 5518–5522.
- von Heijne, G. (1981) *Eur. J. Biochem.* 116, 419–422.
- von Heijne, G., & Blomberg, C. (1979) *Eur. J. Biochem.* 97, 175–181.
- White, S. H., & Wimley, W. (1994) *Curr. Opin. Struct. Biol.* 4, 79–86.
- Wiener, M. C., & White, S. H. (1992) *Biophys. J.* 61, 434–447.
- Yu, Y. G., Thorgeirsson, T. E., & Shin, Y.-K. (1994) *Biochemistry* 33, 14221–14226.
- Yutani, K., Ogasahara, K., Aoki, K., Kakuno, T., & Sugino, Y. (1984) *J. Biol. Chem.* 259, 14076–14081.

BI952300C